Journal of Magnetism and Magnetic Materials 322 (2010) 1912–1916

Contents lists available at ScienceDirect

Journal of Magnetism and Magnetic Materials

journal homepage: www.elsevier.com/locate/jmmm

Low-temperature neutron diffraction study of the crystal and magnetic phase transitions in $DyCrO_4$

Y.W. Long [a], Q. Huang [b], L.X. Yang [a], Y. Yu [a], Y.X. Lv [a], J.W. Lynn [b], Ying Chen [b,c], C.Q. Jin [a,*]

[a] Institute of Physics, Chinese Academy of Sciences, Zhongguancun South Str 3, Beijing, China
[b] NIST Center for Neutron Research, National Institute of Standards and Technology, Gaithersburg, MD 20899, USA
[c] Department of Materials Science and Engineering, University of Maryland, College Park, MD 20742, USA

ARTICLE INFO

Article history:
Received 13 November 2008
Received in revised form
12 December 2009
Available online 21 January 2010

Keywords:
Neutron diffraction
Phase transition
Transition metal oxide

ABSTRACT

The crystal and magnetic structures of $DyCrO_4$ were studied using neutron powder diffraction. Complete diffraction data at 3.6, 17, 27, and 40 K show that a crystal structural phase transition from tetragonal $I4_1/amd$ to orthorhombic *Imma* symmetry is found to take place between 27 and 40 K. This transition does not involve a significant change in the unit cell volume. Strong ferromagnetic reflections are observed at 3.6 and 17 K, and can be fit well using the magnetic model of space group *Im'ma'*, with the moments of both Dy^{3+} and Cr^{5+} ions aligning along the *y*-axis. Detailed temperature dependent magnetic intensities of 101/011 and 211/121 peaks reveal a Curie temperature of T_c=22.35(15) K.

1. Introduction

The mixed rare earth and transition metal oxides have been extensively investigated due to the intriguing physical and chemical properties in structure, magnetism and transport behavior. The family of $RCrO_4$ (R=rare earth) is one of these materials. Except for R=La and Ce, they crystallize into a tetragonal zircon-type structure with $I4_1/amd$ (D_{4h}^{19}, No. 141, Z=4) symmetry at ambient conditions. The zircon-type structure is sensitively dependent on external conditions like temperature and pressure. For example, structural phase transitions from tetragonal to orthorhombic structures have been reported in the zircon-type $TbMO_4$ and $DyMO_4$ (M=Cr, V) materials at low temperatures [1–4]. Generally, at high pressure, the zircon phase will irreversibly evolve toward a tetragonal scheelite structure with space group $I4_1/amd$, accompanying a sharp change (about 10%) in density [5–14].

In addition to the interesting structural properties, the magnetic behavior of $RCrO_4$ is also attractive due to the appearance of the rare Cr^{5+} ions. These compounds provide special structural frameworks to study the magnetic interactions between 3d and 4f electrons. Because of the presence of two different types of magnetic ions (R^{3+} and Cr^{5+}) as well as coupling each other, together with the strong magnetocrystalline anisotropy of the rare earth ions, the magnetic properties of $RCrO_4$ are quite complex. Based on a wide variety of measurements such as magnetization, specific heat, neutron depolarization, and neutron powder diffraction (NPD), ferromagnetic (FM) and antiferromagnetic transitions have been reported for $RCrO_4$ compounds at low temperatures, and several magnetic models were also proposed to obtain good fits to the NPD data [15–21]. It is, therefore, interesting to study the nuclear and magnetic structures of $DyCrO_4$ in detail.

2. Experiment

Because of the thermal instability of $DyCrO_4$ (it decomposes into the refractory $DyCrO_3$ perovskite phase at about 700 °C), it is difficult to obtain single crystal sample. The polycrystalline powder sample with single phase was prepared by solid-state reaction method using highly pure $Dy(NO_3)_3 \cdot 6H_2O$ and $Cr(NO_3)_3 \cdot 9H_2O$ as starting materials [16]. In order to improve the crystallography, an additional annealing procedure in oxygen flow at 300 °C for 6 h was adopted. X-ray diffraction confirmed that the as-made green sample is a pure zircon phase at room temperature.

The neutron powder diffraction experiments were performed using the BT-1 high-resolution powder diffractometer at NIST Center for Neutron Research at temperatures of 3.6, 17, 27, and 40 K. A Cu(3 1 1) monochromator with a wavelength λ=1.540 Å was applied to generate a neutron beam. The NPD data were collected in the 2θ angle range from 3° to 168° with a step of 0.05°. The crystal and magnetic structural parameters were analyzed using the Rietveld full-profile refinements with the GSAS program [22]. In order to determine the magnetic transition

* Corresponding author.
E-mail address: Jin@aphy.iphy.ac.cn (C.Q. Jin).

0304-8853/$ - see front matter © 2010 Elsevier B.V. All rights reserved.
doi:10.1016/j.jmmm.2010.01.006

temperature, the detailed temperature dependence of the magnetic diffraction intensities of 101/011 and 211/121 peaks was carried out on the BT-7 triple axis spectrometer, using a pyrolytic graphite monochromator and filter at a wavelength of 2.36 Å.

3. Results and discussion

Figs. 1(a) and (b) show the refinement results of the NPD data of $DyCrO_4$ at 40 and 27 K, respectively. The observed, calculated, and difference patterns as well as the allowed reflections are presented. For the diffraction spectrum obtained at 40 K, it can be fit well using the zircon-type structural model with space group $I4_1/amd$. In this symmetry, Dy, Cr, and O atoms occupy the special sites 4*a* (0, 3/4, 1/8), 4*b* (0, 1/4, 3/8), and 16*h* (0, *y*, *z*), respectively. The crystal construction is built from CrO_4 tetrahedra with four equal Cr–O bond lengths and DyO_8 dodecahedra. A detailed description of the zircon-type structure was reported in Ref. [13]. Tables 1 and 2 list the refined structural parameters including lattice constants, atomic positions, and selected bond lengths and angles.

Based on the low-temperature X-ray diffraction down to 10 K, a crystal structural phase transition from tetragonal $I4_1/amd$ (No. 141, Z=4) to orthorhombic *Imma* (No. 74, Z=4) symmetry was proposed in $DyCrO_4$ [4]. In our NPD spectra, with temperature decreasing from 40 to 27 K, some diffraction peaks broadened, but

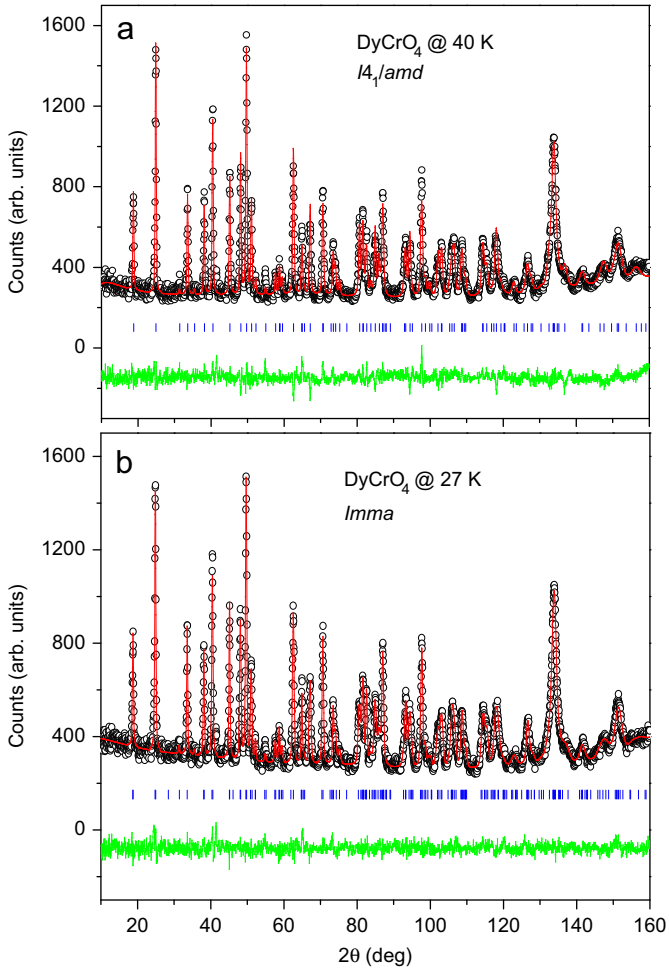

Fig. 1. Observed (○), calculated (solid curve), and difference (below) NPD patterns of $DyCrO_4$ at (a) 40 K and (b) 27 K. Tick marks show the allowed Bragg reflections.

Table 1
Crystal and magnetic structure refinement data for $DyCrO_4$.

T (K)	40	27	17	3.6
NSG	$I4_1/amd$	*Imma*	*Imma*	*Imma*
MSG			*Im'ma'*	*Im'ma'*
Z	4	4	4	4
a (Å)	7.1375(3)	7.1514(4)	7.1599(4)	7.1623(4)
b (Å)		7.1225(4)	7.1147(4)	7.1115(4)
c (Å)	6.2656(3)	6.2650(2)	6.2660(2)	6.2662(2)
V (Å^3)	319.19(3)	319.12(3)	319.19(2)	319.17(3)
Cr_z		0.384(3)	0.377(3)	0.384(2)
O $(1)_y$	0.4325(3)	0.4340(9)	0.4339(6)	0.4336(7)
O $(1)_z$	0.2008(3)	0.2007(12)	0.2001(8)	0.2009(8)
O $(2)_x$		0.8172(8)	0.8169(6)	0.8176(6)
O $(2)_z$		0.5482(12)	0.5477(8)	0.5480(8)
M $(Dy)_y$ (μ_B)			5.54(10)	8.27(12)
M $(Cr)_y$ (μ_B)			0.55(8)	0.79(7)
R_{WP} (%)	6.33	4.34	4.51	5.14
R_P (%)	4.99	3.69	3.62	4.23
χ^2	1.437	1.018	1.318	1.078

NSG=nuclear space group, MSG=magnetic space group.

Table 2
Selected bond lengths (Å) and angles (deg) for CrO_4 and DyO_8 polyhedra.

T (K)	40	27	17	3.6
CrO_4				
Cr–O(1)	1.699(2) (4 ×)	1.742(15) (2 ×)	1.717(14) (2 ×)	1.737(12) (2 ×)
Cr–O(2)		1.664(14) (2 ×)	1.690(13) (2 ×)	1.663(11) (2 ×)
O(1)–Cr–O(1)	114.36(7) (4 ×)	97.5(11)	99.9(10)	97.4(9)
	100.08(13) (2 ×)			
O(1)–Cr–O(2)		114.05(8) (4 ×)	114.12(6) (4 ×)	114.09(8) (4 ×)
O(2)–Cr–O(2)		103.6(11)	101.7(11)	103.6(9)
DyO_8				
Dy–O(1)	2.422(2) (4 ×)	2.425(7) (2 ×)	2.421(4) (2 ×)	2.424(5) (2 ×)
	2.315(2) (4 ×)	2.300(6) (2 ×)	2.298(5) (2 ×)	2.299(5) (2 ×)
Dy–O(2)		2.429(7) (2 ×)	2.434(4) (2 ×)	2.430(5) (2 ×)
		2.319(6) (2 ×)	2.320(4) (2 ×)	2.325(5) (2 ×)

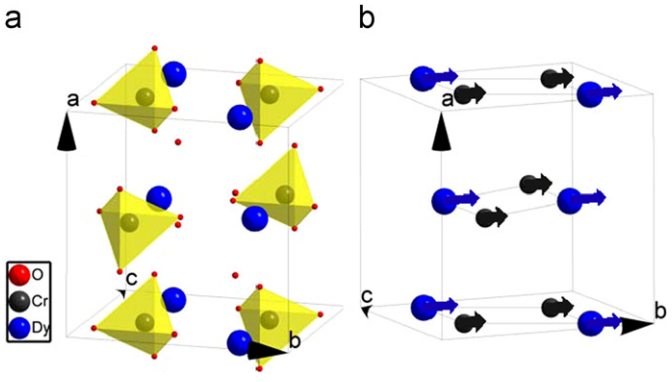

Fig. 2. (a) Crystal (*Imma*) and (b) magnetic (*Im'ma'*) structures of $DyCrO_4$. CrO_4 tetrahedra are shown in (a). The arrows in (b) indicate the spin direction (along the *y*-axis) of Cr^{5+} and Dy^{3+} moments.

no new diffraction peaks were clearly observed. The structural model of *Imma* can give better fitting results than that of $I4_1/amd$ at 27 K. In this new space group, the atomic positions of Dy, Cr, O(1), and O(2) are determined to be 4*e* (0, 1/4, 7/8), 4*e* (0, 1/4, *z*), 8*h* (0, *y*, *z*), and 8*i* (*x*, 1/4, *z*), respectively. Fig. 2(a) represents the correlated schematic structure. CrO_4 and DyO_8 polyhedra still are the basic structural units in *Imma* symmetry. As shown in Table 1,

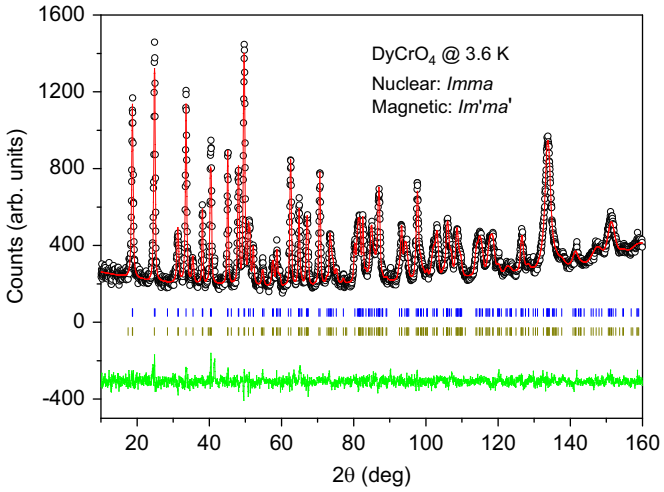

Fig. 3. Observed (○), calculated (solid curve), and difference (below) NPD patterns of $DyCrO_4$ at 3.6 K. The tick marks in the first and the second lines represent the allowed nuclear and magnetic Bragg reflections, respectively.

there is no significant change ($<0.03\%$) in unit cell volume associated with the structural transition. Moreover, for the positions of cations, only a slight shift of chromium (from 0.375 to 0.384) takes place along the *z*-axis direction. Therefore, the low-temperature structural transition that occurred in $DyCrO_4$ most probably is of second-order. This transition is attributed to the pseudo Jahn–Teller effects due to the splitting of the accidental orbital degeneracy or near-degeneracy in crystal field levels [23]. Similarly, a second-order structural transition from tetragonal to orthorhombic symmetry was also claimed in the isostructural compound $TbCrO_4$ [1]. It was reported that an anomaly in specific heat occurred in $DyCrO_4$ at ~31 K owing to the presence of this structural phase transition [4]. However, no magnetic anomaly is observed around this temperature according to previous magnetic measurements as well as present NPD experiments.

Fig. 3 shows the NPD spectrum taken at 3.6 K as well as the refinement results. Obviously, there is a considerable change in the relative intensities of the diffraction peaks in this spectrum with respect to the diffraction pattern obtained at 27 K. If only the nuclear model of *Imma* is used to fit the experimental data, there

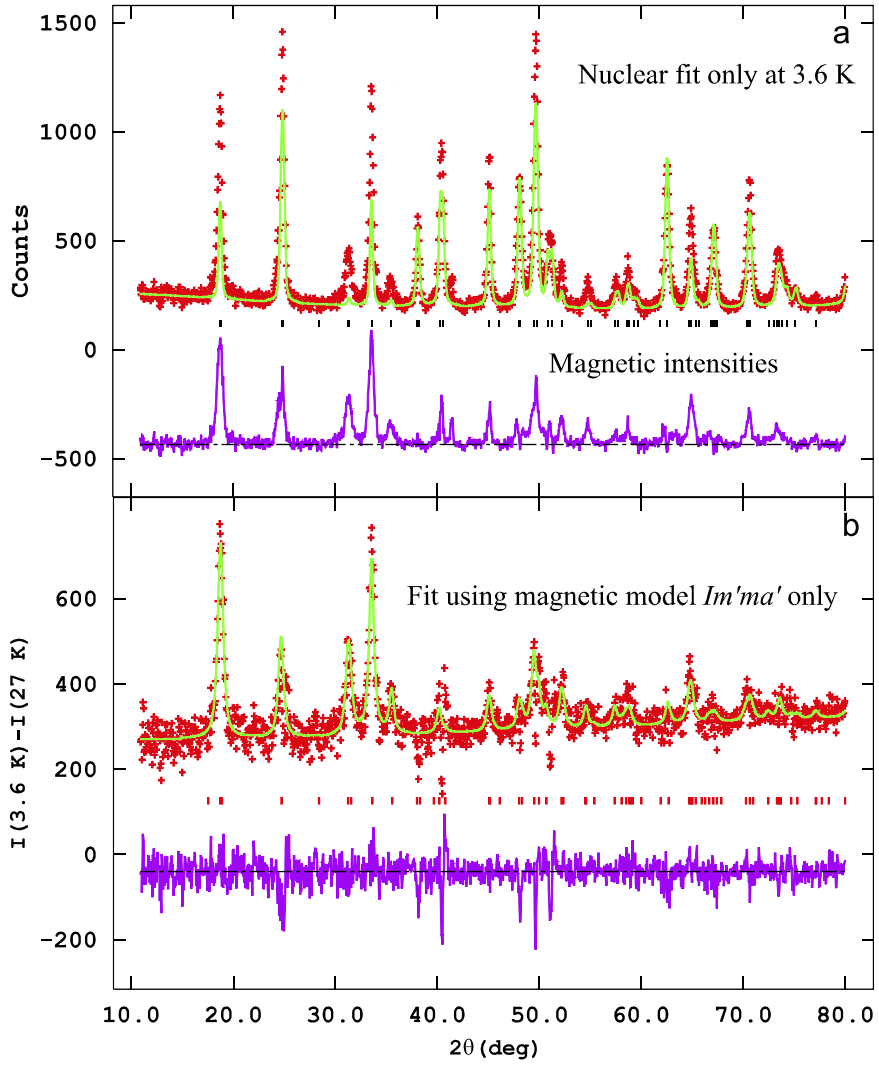

Fig. 4. (a) Nuclear fit (solid curve) to the NPD data (○) at 3.6 K in scattering angle range 10–80°. The difference (below) indicates the magnetic reflections. Tick marks show the allowed Bragg reflections. (b) Magnetic fit (solid curve) to the magnetic reflections (○) at 3.6 K. The difference is shown in the bottom. Tick marks show the allowed magnetic Bragg reflections.

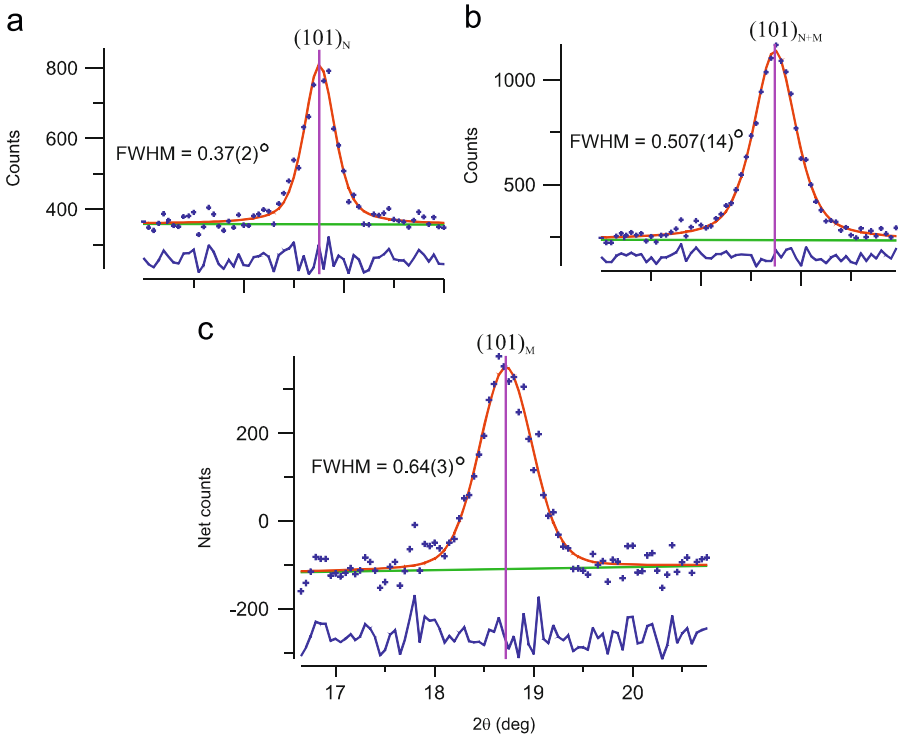

Fig. 5. Full width at half maximum of the 101/011 peaks (a) nuclear reflections at 27 K, (b) nuclear and magnetic reflections at 3.6 K, and (c) net magnetic reflections at 3.6 K.

is a large difference between experiment and calculation. Fig. 4(a) shows the difference in lower angle range from 10° to 80°. A paramagnetic to FM transition has been reported in $DyCrO_4$ at ~23 K based on the magnetic and specific heat measurements [4], and these features are indeed indicative of the presence of magnetic reflections. Our NPD data collected at 3.6 K can be fit well using the nuclear model of *Imma* together with a simple FM model (propagation vector $\boldsymbol{\kappa}$=(0, 0, 0)) of *Im'ma'*, as shown in Fig. 3. In this magnetic model, both the Cr^{5+} and Dy^{3+} spin moments collinearly align along the *y*-axis direction. According to this magnetic space group, the magnetic structure of $DyCrO_4$ is plotted in Fig. 2(b), where only magnetic ions are presented. According to the refined results, the shortest distance between magnetic ions is Cr^{5+}–Dy^{3+} in the planes perpendicular to the *a*-axis at *a*=0 or 0.5. Therefore, the magnetic interactions between Cr^{5+} and Dy^{3+} ions should be mainly responsible for the FM transition of $DyCrO_4$, as Buisson et al. [1] reported for the FM origin of the isostructural $TbCrO_4$ system. The values of the magnetic moments are determined to be 0.79 and 8.27 μ_B for Cr^{5+} and Dy^{3+} at 3.6 K, respectively, as listed in Table 1. Both moments are close to the free-ion values of 1.0 μ_B for Cr^{5+} and 10.0 μ_B for Dy^{3+} ions.

To identify the magnetic scattering, the NPD data collected at 27 K, where all the Bragg peaks are structural in origin, are subtracted from the neutron data obtained at 3.6 K, in the ordered magnetic state. For unpolarized neutrons, this subtraction technique should yield the magnetic Bragg peaks if there is no significant structural distortion associated with the phase transition (so the nuclear peaks do not change intensity significantly) [24]. Fig. 4(b) shows the results of this subtraction for scattering angles 10–80°. These strong magnetic reflections clearly confirm the long-range FM ordering in the sample, and can be fit well by the ferromagnetic model of *Im'ma'*.

Fig. 5 represents the full width at half maximum (FWHM) of the 101/011 peaks. Because the unit cells for the nuclear and magnetic structure are identical in $DyCrO_4$, both the nuclear and magnetic reflections are responsible for the diffraction intensity of 101/011 peaks. In addition, the orthorhombic distortion only leads to a slight separation (<0.051 Å) between the *a*- and the *b*-axis. The 101 and 011 diffraction peaks cannot be resolved in our experiment, but the FWHM of the overlapping 101/011 peaks increases from 0.37(2)° to 0.507(14)°, while the corresponding intensity approximately doubles when the temperature decreases from 27 to 3.6 K. This means that the orthorhombic distortion increases with decrease in temperature. After subtracting the nuclear diffraction contribution, the net magnetic diffraction of 101/011 peaks at 3.6 K is obtained as shown in Fig. 5(c). The magnetic intensity is comparable to the nuclear-only scattering, whereas the magnetic peak is significantly broader (FWHM of 0.64(3)°), suggesting a modest FM domain size.

In order to determine the onset of the FM order, the temperature dependence of diffraction intensities of 101/011 and 211/121 peaks was measured as shown in Fig. 6. The 101/011 peaks were measured on warming and cooling and no evidence of any thermal hysteresis was observed in these data, indicating that the transition is continuous in nature. The curves in the figure are the result of fitting the data using mean field theory, to obtain an estimate of the ordering temperature of 22.4 K, in good agreement with magnetization and specific heat measurement results [4]. No other transitions are evident in these data.

4. Conclusion

In summary, we have studied the low-temperature crystal and magnetic structural phase transitions of $DyCrO_4$ using high-

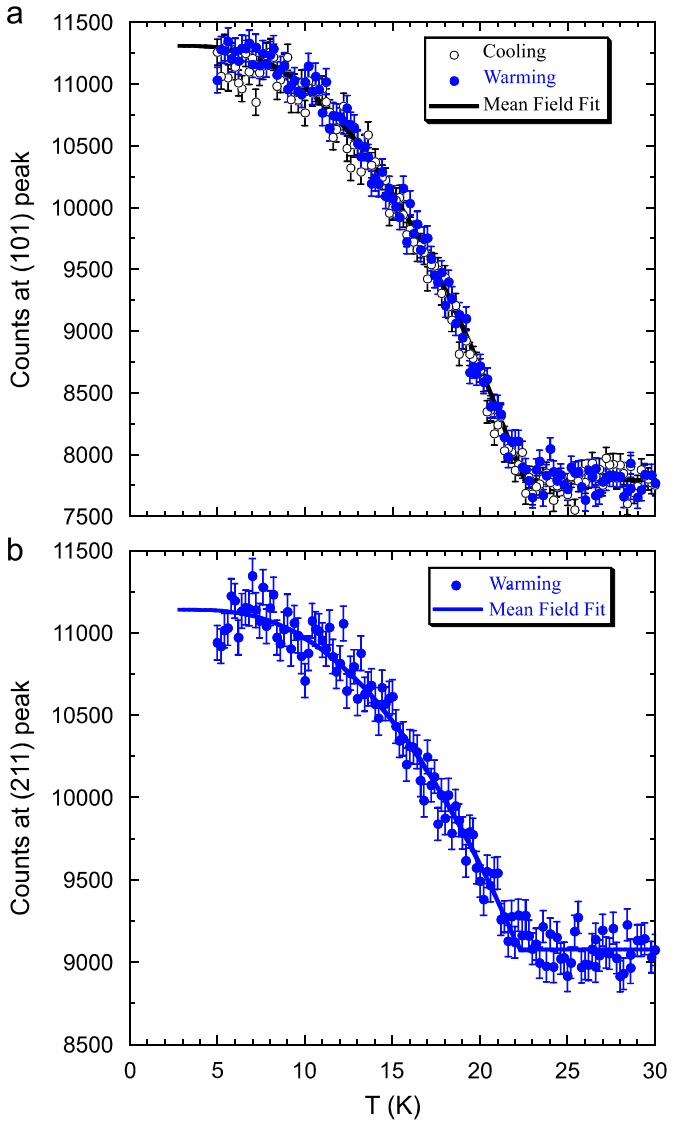

Fig. 6. Temperature dependence of intensity of (a) 101/011 and (b) 211/121 peaks. The solid curves are fits using mean field theory to determine the Curie temperature to be 22.4 K. The data in (a) were taken on both warming and cooling, and the continuous nature of the measurements and the lack of any hysteresis indicate that the magnetic transition is second order.

resolution neutron powder diffraction. A tetragonal to orthorhombic crystal structural transition was determined between 40 and 27 K due to the pseudo Jahn–Teller effects in crystal field levels, accompanying the reduction of symmetry from $I4_1/amd$ (No. 141, Z=4) to $Imma$ (No. 74, Z=4). Long-range ferromagnetic order develops below 22.4 K, and the data can be fit well with the FM model of *Im'ma'*. In this model the magnetic and chemical unit cells are equal and the Cr^{5+} and Dy^{3+} magnetic moments are collinear and point along the *b*-axis.

Acknowledgement

This work was supported by NSF & MOST of China through research projects.

References

[1] G. Buisson, F. Tcheou, F. Sayetat, K. Scheunemann, Solid State Commun. 18 (1976) 871.
[2] M. Steiner, H. Dachs, H. Ott, Solid State Commun. 29 (1979) 231.
[3] R.T. Harley, W. Hayes, S.R.P. Smith, Solid State Commun. 9 (1971) 515.
[4] K. Tezuka, Y. Hinatsu, J. Solid State Chem. 160 (2001) 326.
[5] K. Kusaba, T. Yagi, M. Kikuchi, Y. Syono, J. Phys. Chem. Solids 47 (1986) 675.
[6] A. Jayaraman, G.A. Kourouklis, G.P. Espinosa, A.S. Cooper, L.G. Van Uitert, J. Phys. Chem. Solids 48 (1987) 755.
[7] X. Wang, I. Loa, K. Syassen, M. Hanfland, B. Ferrand, Phys. Rev. B 70 (2004) 064109.
[8] E. Knittle, Q. Williams, Am. Mineral. 78 (1993) 245.
[9] W.V. Westrenen, M.R. Frank, J.M. Hanchar, Y. Fei, R.J. Finch, C.S. Zha, Am. Mineral. 89 (2004) 197.
[10] Y.W. Long, W.W. Zhang, L.X. Yang, Y. Yu, R.C. Yu, S. Ding, Y.L. Liu, C.Q. Jin, Appl. Phys. Lett. 87 (2005) 181901.
[11] Y.W. Long, L.X. Yang, S.J. You, Y. Yu, R.C. Yu, C.Q. Jin, J. Liu, J. Phys.: Condens. Matter 18 (2006) 2421.
[12] Y.W. Long, L.X. Yang, Y. Yu, F.Y. Li, R.C. Yu, S. Ding, Y.L. Liu, C.Q. Jin, Phys. Rev. B 74 (2006) 054110.
[13] Y.W. Long, L.X. Yang, Y. Yu, F.Y. Li, R.C. Yu, C.Q. Jin, Phys. Rev. B 75 (2007) 104402.
[14] Y.W. Long, L.X. Yang, Y. Yu, F.Y. Li, Y.X. Lu, R.C. Yu, Y.L. Liu, C.Q. Jin, J. Appl. Phys. 103 (2008) 093542.
[15] E. Jimenez, J. Isasi, R.S. Puche, J. Alloys Compd. 312 (2000) 53.
[16] R.S. Puche, E. Jimenez, J. Isasi, M.T.F. Diaz, J.L.G. Munoz, J. Solid State Chem. 171 (2003) 161.
[17] T. Keitaro, D. Yoshihiro, H. Yukio, J. Mater. Chem. 12 (2002) 1189.
[18] E. Jimenez, J. Isasi, R.S. Puche, J. Solid State Chem. 164 (2002) 313.
[19] E. Jimenez, J. Isasi, M.T. Fernandez, R.S. Puche, J. Alloys Compd. 344 (2002) 369.
[20] E. Jimenez, P. Bonville, J.A. Hodges, P.C.M. Gubbens, J. Isasi, R.S. Puche, J. Magn. Magn. Mater. 272 (2004) 571.
[21] E.J. Melero, N.H. Van Dijk, W.H. Kraan, P.C.M. Gubbens, J. Isasi, R.S. Puche, J. Magn. Magn. Mater. 288 (2005) 1.
[22] A.C. Larson, R.B. Von Dreele, Los Alamos National Laboratory Report No. LAUR 86–748, 2004 (unpublished).
[23] G.A. Gehring, K.A. Gehring, Rep. Prog. Phys. 38 (1975) 1.
[24] H. Zhang, J.W. Lynn, W.-H. Li, T.W. Clinton, D.E. Morris, Phys. Rev. B 41 (1990) 11229.